

# Bmal1 Attenuates Collagen-Induced Arthritis by Regulating Macrophage Polarization via Sirt1

Lu Ye<sup>1</sup>, Xiaomei Wang<sup>2</sup>, Weihong Xu<sup>1,\*</sup>, Huaxiang Wu<sup>1,\*</sup>

<sup>1</sup>Department of Rheumatology, The Second Affiliated Hospital of Zhejiang University School of Medicine, Hangzhou, 310009, People's Republic of China;

<sup>2</sup>Department of Pathology, The Second Affiliated Hospital of Zhejiang University School of Medicine, Hangzhou, 310009, People's Republic of China

\*These authors contributed equally to this work

Correspondence: Weihong Xu; Huaxiang Wu, Email 2314003@zju.edu.cn; wuhx8855@zju.edu.cn

**Background:** Rheumatoid arthritis (RA) is an inflammatory disease primarily affecting the joints, with macrophages playing a critical role in its pathogenesis. Bmal1 is a key regulator of macrophage polarization, but its role in RA remains unclear. This study aimed to define the role of Bmal1 in regulating macrophage polarization in RA and to elucidate the underlying molecular mechanisms.

**Methods:** Synovial tissue and peripheral blood mononuclear cells (PBMCs) were used to assess Bmal1 expression. High-throughput transcriptome sequencing was performed to identify signaling pathways and key molecules in RAW264.7 cells following Bmal1 knockdown. The expression of Bmal1, macrophage polarization markers and pro-inflammatory cytokines was evaluated using quantitative real-time PCR, immunofluorescence, Western blotting, flow cytometry and ELISA.

**Results:** Bmal1 expression was significantly reduced in RA patients, which was confirmed by the Gene Expression Omnibus (GEO) datasets GSE55235. Methotrexate (MTX) treatment was associated with increased Bmal1 expression. In vitro, Bmal1 overexpression inhibited M1 macrophage polarization and NF- $\kappa$ B signaling. Mechanistically, the JASPAR database predicted that Bmal1 binds to the Sirt1 promoter, which was confirmed by chromatin immunoprecipitation (ChIP) and dual-luciferase reporter assays. Bmal1 positively regulated Sirt1 expression in RAW264.7 cells. Sirt1 knockdown partially reversed the inhibition of M1 macrophage polarization and NF- $\kappa$ B signaling induced by Bmal1 overexpression. In vivo, Bmal1 expression was reduced in collagen-induced arthritis (CIA) mice, whereas its overexpression attenuated disease severity and was associated with increased Sirt1 expression and enhanced M2 macrophage polarization.

**Conclusion:** Bmal1 attenuates inflammatory responses by regulating macrophage polarization, potentially through up-regulation of Sirt1 and inhibition of NF- $\kappa$ B signaling. These findings suggest that Bmal1 may represent a potential therapeutic target for RA.

**Keywords:** Bmal1, rheumatoid arthritis, macrophage polarization, Sirt1, NF- $\kappa$ B signaling pathway

## Introduction

Rheumatoid arthritis (RA), a leading cause of disability worldwide, is a chronic systemic autoimmune disease characterized by persistent synovitis and systemic inflammation.<sup>1</sup> Current therapies such as disease-modifying anti-rheumatic drugs and biological agents including anti-tumor necrosis factor-alpha inhibitor (TNF- $\alpha$ i) and interleukin-6 inhibitor (IL-6i) have significantly improved clinical outcomes and quality of life.<sup>2</sup> However, for refractory RA patients, current therapeutic approaches are inadequate to prevent the progression of the disease, underscoring the urgent need for new treatment strategies. Moreover, the development of effective treatments is limited by an incomplete understanding of the underlying molecular mechanisms.

Although the etiology of the synovitis in RA remains largely unknown, it is well-established that the disease is immune-mediated. Macrophage polarization plays a crucial role in RA,<sup>3</sup> as macrophages are key antigen-presenting cells (APCs) that influence immune responses by releasing cytokines and growth factors.<sup>4,5</sup> Macrophages can be categorized into two phenotypes, commonly known as M1 and M2. M1 phenotype is an inflammatory state, characterized by high expression of MHC-II, CD80, CD86, CD38 and TLR4, which enhances the production of pro-inflammatory cytokines

including IL-1 $\beta$ , IL-6 and TNF- $\alpha$ . M2 macrophages, characterized by the expression of CD163, CD204, CD206 and MerTK, are anti-inflammatory cells that facilitate tissue repair and promote resolution of inflammation.<sup>6,7</sup> In RA, an imbalance between these phenotypes, particularly the predominance of M1 macrophages, contributes to persistent inflammation, pannus formation and joint damage.<sup>8</sup> Although macrophage polarization is recognized as a key factor in RA pathogenesis, the precise regulatory mechanisms underlying this process remain unclear.

Interestingly, RA is characterized by circadian rhythm disturbances, with morning stiffness being a hallmark symptom. Inflammatory cytokines that contribute to joint stiffness are often elevated in the morning, highlighting the circadian nature of the disease.<sup>9,10</sup> The circadian rhythm is controlled by a network of clock genes including brain and muscle Arnt-like protein-1 (Bmal1), circadian locomotor output cycles kaput (Clock), Period (Per), and Cryptochrome (Cry).<sup>11</sup> Emerging evidence suggests that the circadian system regulates various inflammatory processes, and disruptions to circadian genes have been linked to the increased incidence of RA.<sup>12,13</sup> Notably, while fibroblasts exhibit normal circadian rhythms, primary synovial fibroblasts from RA patients show impaired rhythmicity.<sup>14</sup>

Bmal1, a core circadian clock gene, plays roles beyond the regulation of daily transcriptional rhythms and is implicated in various diseases, including alcoholic liver disease,<sup>15</sup> atherosclerosis,<sup>16</sup> diabetes<sup>17</sup> and RA.<sup>18</sup> Myeloid-specific Bmal1 knockout impairs mitochondrial function in macrophages and exacerbates inflammatory injury.<sup>19</sup> In alcoholic liver disease, Bmal1 interacts with S100A9 to inhibit macrophage glycolysis and M1 polarization.<sup>20</sup> Collectively, these findings suggest that Bmal1 may exert protective effects by regulating macrophage function. Sirt1, a NAD<sup>+</sup>-dependent deacetylase, is a key regulator of NF- $\kappa$ B signaling and macrophage polarization, exerting anti-inflammatory and cytoprotective effects through deacetylation of p65.<sup>21</sup> These protective roles have been demonstrated across multiple organs, including the liver, lung and kidney.<sup>21–23</sup> Notably, Sirt1 exhibits circadian oscillations, suggesting potential crosstalk with clock genes.<sup>24</sup> Therefore, we hypothesize that Bmal1 may modulate macrophage polarization via the Sirt1/NF- $\kappa$ B axis.

However, the role of Bmal1 in RA and its underlying mechanisms remain unclear, partly due to conflicting reports regarding its expression. While one study reported that Bmal1 was down-regulated in RA synovial tissues,<sup>25</sup> others have observed increased Bmal1 expression in synovial tissues from RA patients<sup>26</sup> and in TNF- $\alpha$ -stimulated human synovial fibroblasts.<sup>27</sup> To address these discrepancies, we employed a collagen-induced arthritis (CIA) model and RAW264.7 cells to investigate the effects of Bmal1 on macrophage polarization and to elucidate the underlying molecular mechanisms.

## Materials and Methods

### Sample Collection and Human Ethics

Synovial tissue samples were obtained from RA (n=8) and knee OA (n=10) patients as part of their medical management in the Orthopedics department of the Second Affiliated Hospital of Zhejiang University School of Medicine between May 9, 2025 and October 3, 2025. Peripheral blood mononuclear cells (PBMCs) from RA patients (n = 6) were collected in the Department of Rheumatology between May 15, 2025 and October 5, 2025 before initiation of methotrexate (MTX) monotherapy and after three months of treatment (15–20 mg/week). Following isolation, PBMCs were immediately lysed in TRIzol reagent (Invitrogen) and stored at –80°C. After completion of sample collection, total RNA was extracted from all samples in a single batch to minimize batch effects. Ethical approval was obtained from the Ethics Committee of the Second Affiliated Hospital of Zhejiang University School of Medicine (approval number: 2025–0681). All subjects signed an informed consent form. All of the RA patients fulfilled the 1987 and 2010 American College of Rheumatology diagnostic criteria for RA.<sup>28,29</sup> The knee OA patients met the 1986 American College of Rheumatology (ACR) classification criteria for OA.<sup>30</sup> The studies in this work abide by the Declaration of Helsinki principles.

### Data Collection

The RA dataset GSE55235 was obtained from the GEO database (<https://www.ncbi.nlm.nih.gov/geo>). Differentially expressed genes (DEGs) between RA and healthy control were identified using the “Limma” package in R language, with screening threshold of adj.P < 0.05, |log2FC| > 1. The CIBERSORT algorithm was used to assess the immune cell infiltration in the RA group and the control group. Subsequently, the relationship between Bmal1 and macrophage

polarization markers was evaluated by Spearman correlation analysis. The JASPAR database (<https://jaspar.elixir.no/>) was employed to predict the interactions between transcription factors and their target genes.

## Collagen-Induced Arthritis (CIA) Mice and Bmal1 Overexpression Treatments

Male DBA/1 mice (5–6 weeks old) were purchased from Jiangsu Jicui Medicine Biotechnology Co., Ltd. All mice were acclimated for 1 week prior to experimentation. Subsequently, the mice were randomly assigned to three groups (n = 5 per group): normal control (Sham), CIA model (CIA+NC) and CIA model with Bmal1 overexpression (CIA+OE-Bmal1) ([Supplemental methods](#)). The CIA model was established using the methodology previously described.<sup>31</sup> Briefly, CIA model was induced as follows. Bovine type II collagen was emulsified with complete Freund's adjuvant. Mice were anesthetized with 2% isoflurane, and 100  $\mu$ L of the prepared emulsion was then administered intradermally at the base of the tail per mouse, except in the Sham group. On day 21, a booster injection of 100  $\mu$ L of emulsion was administered. Meanwhile, the lentivirus carrying Bmal1 or a negative control (NC) was based on the pLVX-pGK-puro vector driven by the CMV promoter, with a titer of  $1.80 \times 10^9$  transducing units (TU)/mL. After dilution, each mouse received 100  $\mu$ L of the viral suspension via injection, corresponding to a dose of  $2.5 \times 10^7$  TU per mouse. Mice received an intraperitoneal injection of 2.5% tribromoethanol (0.2 mL/10 g). Once a surgical plane of anesthesia was achieved, blood was collected through orbital bleeding, followed by euthanasia via cervical dislocation. The experiment was approved by Ethics Committee of the Second Affiliated Hospital of Zhejiang University School of Medicine, Hangzhou, China (approval number: 2024–184).

## Evaluation of the Severity of Arthritis

Investigators were blinded to group allocation during clinical scoring. The arthritis scores were evaluated using a 5-point scale:<sup>32</sup> 0 = normal paw with no erythema or swelling, 1 = mild swelling and redness of the paw or one digit, 2 = two joints involved, 3 = more than two joints involved, 4 = swelling from the entire paw to ankle joints. Each mouse received an arthritis score that represented the sum of all paws, with a maximum score of 16.

## Histopathological Analysis

The knees were collected and fixed with 10% formalin after the mice were sacrificed. Then, 5  $\mu$ m sections were stained with haematoxylin and eosin (HE). Investigators were blinded to group allocation during histological evaluation. The histopathological changes including synovial hyperplasia, inflammatory cell infiltration, as well as cartilage and bone erosion were observed with an Olympus BX53 microscope.

## Cell Culture

RAW264.7 cell line was obtained from Procell. Cells were cultured in Dulbecco's modified eagle medium (DMEM, Gibco) at the temperature of 37 °C in 5% CO<sub>2</sub> with 10% fetal bovine serum (FBS, Gibco), 100 U/mL penicillin and 100  $\mu$ g/mL streptomycin. RAW264.7 cells were treated with 100 ng/mL LPS or 10 ng/mL IL4 to induce differentiation.

## Mouse Bmal1 Plasmid Construction

The Bmal1 overexpressed plasmid (Bmal1-OE) was obtained from Ribobio. Overexpression of Bmal1 was achieved by transfection with Bmal1-OE, and empty vector was employed as the negative control. Plasmids were then transfected into RAW264.7 cells and Bmal1 mRNA expression was verified by qRT-PCR.

## RNA Interference

Lipofectamine 2000 reagent (Invitrogen) was used to interfere RNA according to instructions. Small interfering RNA (siRNA) oligonucleotides against Bmal1 were synthesized by Ribobio. Meanwhile, a scrambled siRNA was used in as a negative control. RAW264.7 cells were cultured in DMEM medium for 12 h. Then the siRNA-Bmal1 or the scrambled siRNA was introduced into RAW264.7 cells.

## Quantitative Real-Time PCR

Total RNA was extracted by Trizol reagents in terms of the manufacturer's instructions. Reverse transcription of total RNA was performed by using HiScript<sup>®</sup> II Q Select RT SuperMix for qRT-PCR (Vazyme Biotech Co.,Ltd). Then, qRT-PCR was performed by using 2\*Q3 SYBR qPCR Master Mix (TOLOBIO) in a ViiA 7 Real-Time PCR machine (Thermo Fisher Scientific). The  $\beta$ -actin gene was used as an internal reference gene. The mRNA expression levels were assessed by the  $2^{-\Delta\Delta Ct}$  method and normalized to  $\beta$ -actin expression. Primer sequences are listed in [Supplementary Table 1](#).

## Western Blot Analysis

Protein extracts were performed by using the RIPA lysis buffer and protein concentration was determined using a BCA protein assay kit (Beyotime Institute of Biotechnology). Then protein samples were electrophoreted on sodium dodecyl sulfate-polyacrylamide gel electrophoresis (SDS-PAGE) and transferred onto polyvinylidene difluoride (PVDF) membrane. The resulted membrane was washed and incubated with 5% blotting grade blocker (Bio-Rad) for 1 h at room temperature. Then, the membrane was incubated with appropriate primary antibodies at 4 °C overnight, followed by secondary antibody for 2 h. The signals were detected using an enhanced chemiluminescence (ECL) detection reagent (Applygen, P1050). The membranes were exposed to X-ray films (Carestream Health, 6535876) in a darkroom, followed by standard development and fixation procedures. The resulting films were scanned using a CanoScan scanner (Canon LIDE 300). The following primary antibodies were used: anti- $\beta$ -actin (Cat T0022, Affinity), anti-Bmal1 (Cat sc-365645, Santa), anti-NOS2 (Cat 22226-1-AP, Proteintech), anti-Sirt1 (Cat Ab12193, Abcam), anti-p65 (Cat 8242, Cell Signaling Technology), anti-p-p65 (Cat 3033, Cell Signaling Technology). Details of the antibodies are listed in [Supplementary Table 2](#).

## Immunofluorescence Staining

To minimize nonspecific binding, tissue sections were blocked with 5% normal goat serum (Invitrogen). Immunostaining was performed by using primary antibodies and corresponding secondary antibodies. Nuclei were counterstained with DAPI (Beyotime Institute of Biotechnology). The stained sections were observed under a fluorescence microscope (Olympus BX53). Details of the antibodies are provided in [Supplementary Table 2](#).

## Cytokines Detections

The levels of IL-1 $\beta$ , IL-6 and TNF- $\alpha$  were detected using the commercial assay kits (Elabscience) according to the manufacturer's guidelines.

## Flow Cytometric Analysis

Cells ( $1 \times 10^6$  per sample) were resuspended in PBS containing 0.5% bovine serum albumin (BSA) and incubated with anti-CD16/32 antibody for Fc receptor blocking. Cells were then stained with fluorochrome-conjugated antibodies against CD86 and CD206 at 4°C for 30 min in the dark. After washing, cells were resuspended in PBS and analyzed using a Beckman Coulter CytoFLEX flow cytometer. Data were analyzed using CytExpert software (version 2.4). The gating strategy was applied as follows. Cells were first gated based on forward and side scatter (FSC/SSC) to exclude debris, followed by FSC-A versus FSC-H gating to exclude doublets. Autofluorescence was assessed using unstained cells, and positive populations for each marker (CD86 or CD206) were defined based on isotype control staining. The percentages of CD86<sup>+</sup> and CD206<sup>+</sup> cells were calculated using single-parameter histograms.

## Dual-Luciferase Reporter Gene Assay

RAW264.7 cells were transfected with PLG-Sirt1 plasmid, PLG-Sirt1-Mut plasmid or PLG plasmid with Bmal1 plasmid or negative control plasmid. The ratio of firefly luciferase activity to Renilla luciferase activity was analyzed. Cells were collected 48 h after transfection and analyzed using a dual-luciferase reporter system (Promega).

## Chromatin Immunoprecipitation (ChIP) Assays

The EpQuik Chromatin Immunoprecipitation (ChIP) Kit was purchased from Epigentek. ChIP assays were performed according to the manufacturer's instructions. Briefly, cells were cross-linked with 1% formaldehyde for 10 min at room temperature with gentle rotation. The cross-linking reaction was quenched by adding 1 mL of 1.25 M glycine. Chromatin was subsequently sheared using a JY92-IIN ultrasonic cell disruptor (Ningbo Scientz Biotechnology) equipped with a  $\Phi 6$  mm probe. Sonication was performed at a power of 90 W with cycles of 1.8s on and 10s off, for a total duration of 20 min (effective sonication time: 3.6 min), under continuous cooling in a 4°C water bath. To verify chromatin fragmentation, 50  $\mu$ L of the sheared sample was subjected to reverse cross-linking, followed by electrophoresis on a 1.5% agarose gel. The DNA fragments were predominantly distributed in the range of 150–500 bp. Immunoprecipitation was then carried out using an anti-Bmal1 antibody or normal IgG as a negative control to enrich protein–DNA complexes. The purified DNA was subsequently analyzed by ChIP-qPCR. ChIP-qPCR primers were designed to target the promoter region of the gene of interest (from –2000 bp to 0 bp relative to the transcription start site). The primer sequences were as follows: forward: CAGACTCCTCCAACCCGTAA; reverse: GGACACAGACGAAAATCTG, generating a 156 bp amplicon. Each sample was analyzed in triplicate, and relative enrichment was calculated using the  $2^{-\Delta\Delta C_t}$  method.

## Statistical Analysis

Statistical analysis was performed by using the SPSS version 16.0 software. GraphPad Prism 9.5 was used to draw diagrams. The sample size (n) represents independent biological replicates. All data were expressed as mean  $\pm$  standard error of the mean (SEM). Normality of data distribution was assessed using the Shapiro–Wilk test, and homogeneity of variances was evaluated using Levene's test. For comparisons between two groups, a Student's *t*-test was applied. For multiple group comparisons, one-way analysis of variance (ANOVA) followed by Tukey's post hoc test was used. Effect sizes were assessed using Cohen's *d*, where *d*=0.2 is considered as a small effect, *d*=0.5 as a medium effect and *d*=0.8 as a large effect. A *p* value <0.05 was considered statistically significant.

## Results

### Bmal1 is Down-Regulated in RA Patients

Synovial tissues from RA (n=8) and OA (n=10) patients were collected to detect Bmal1 expression. Clinical and laboratory features of RA and OA patients were shown in [supplementary Table 3](#). Among the 8 RA patients, 5 were receiving methotrexate, 3 leflunomide, 2 glucocorticoid, and 1 patient each hydroxychloroquine, iguratimod or salazosulfapyridine at the time of sample collection, with some patients received combination therapy. As shown in [Figure 1A](#), the mRNA expression of Bmal1 in RA synovial tissues was significantly decreased, suggesting a potential role of Bmal1 in the pathogenesis of RA. Additionally, we observed a significant negative correlation between Bmal1 expression and key indicators of RA disease activity including disease activity score of 28 joints (DAS28-CRP), C-reactive protein (CRP) and erythrocyte sedimentation rate (ESR) ([Figure 1B](#)). Interestingly, MTX treatment was associated with increased Bmal1 expression in PBMCs from RA patients (n=6), with a large effect size (Cohen's *d* = 2.12) ([Figure 1C](#)). Clinical and laboratory features of RA patients were shown in [supplementary Table 4](#). The RA dataset GSE55235 was obtained from the GEO database and Bmal1 expression in RA and healthy control were analyzed. The results showed a significant decrease in Bmal1 expression in RA synovial tissues compared to healthy controls ([Figure 1D](#)). Immune cell infiltration analysis showed an increased proportion of M0 macrophages in RA synovial tissues compared with controls ([Figure 1E](#)), although the difference was not statistically significant. Specifically, a moderate positive correlation between Bmal1 expression and M2 marker scores was observed in controls (*r*=0.48), whereas this relationship was attenuated and became slightly negative in RA (*r*=–0.08), suggesting a potential shift in association ([Figure 1F](#)). Although these correlations did not reach statistical significance, these findings provide exploratory evidence for a potential association between Bmal1 and macrophage polarization.

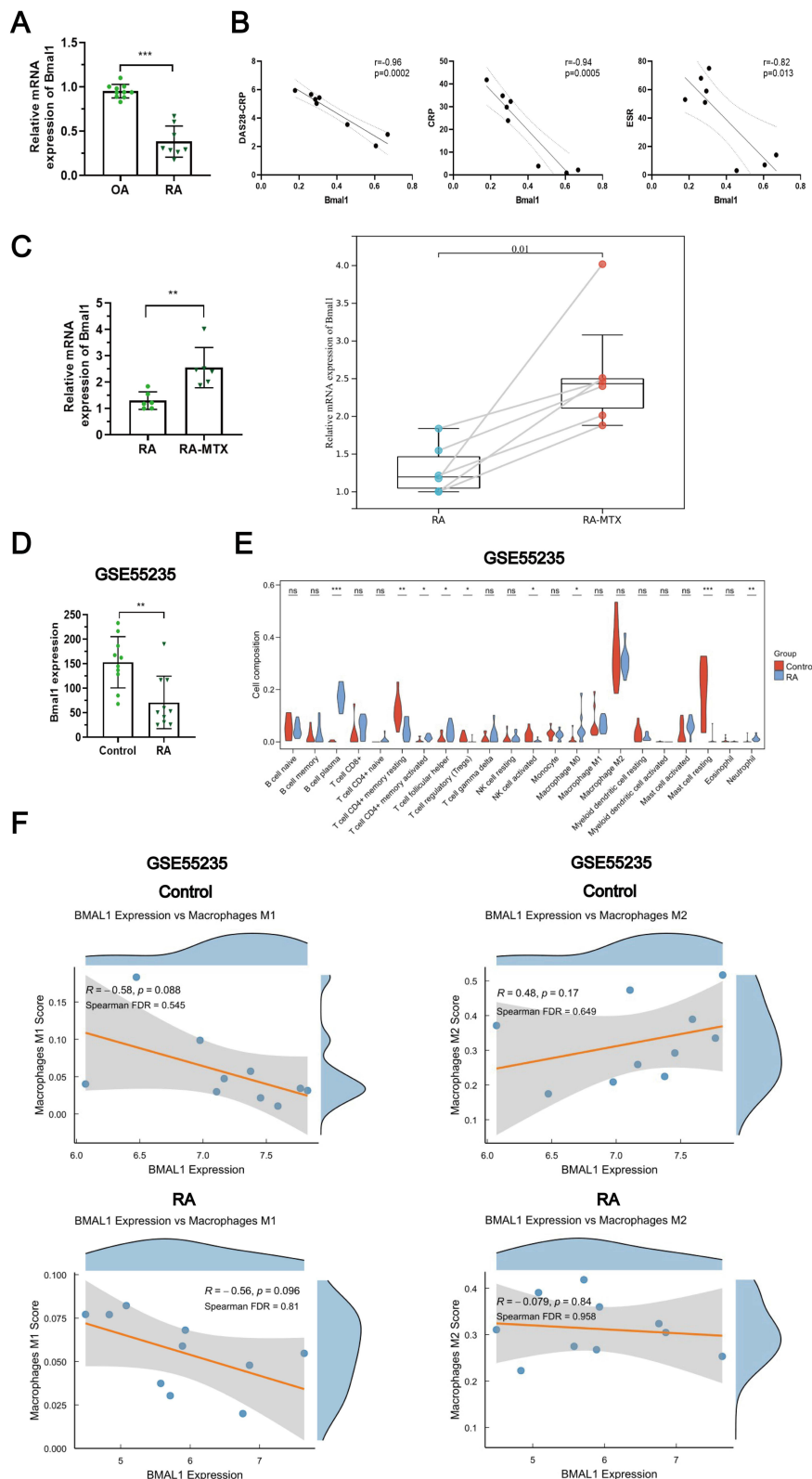


**Figure 1** Bmal1 is down-regulated in RA patients. **(A)** Relative mRNA expression of Bmal1 in synovial tissues from RA patients (n=8) and OA (n=10) patients. **(B)** Relationship between Bmal1 mRNA expression and DAS28-CRP, CRP and ESR in RA patients were analyzed by Spearman correlation analysis. **(C)** Relative mRNA expression of Bmal1 in PBMCs from RA patients (n=6) before and after MTX treatment. **(D)** The dataset GSE55235 was obtained from the GEO database and Bmal1 expression in RA patients and the healthy controls was analyzed. **(E)** Immune cell infiltration analysis of dataset GSE55235. **(F)** Correlations between M1/M2 marker scores and Bmal1 expression in RA patients and healthy controls from the GSE55235 dataset were analyzed using Spearman correlation. Experiments in A and C were performed with 3 technical replicates. Data are presented as the mean  $\pm$  SEM. \* $P < 0.05$ , \*\* $P < 0.01$ , \*\*\* $P < 0.001$ . P values  $< 0.05$  were considered significant.

**Abbreviations:** Bmal1, brain and muscle Arnt-like protein-1; CRP, C-reactive protein; DAS28, disease activity score of 28 joints; ESR, erythrocyte sedimentation rate; OA, osteoarthritis; PBMCs, peripheral blood mononuclear cells; RA, rheumatoid arthritis.

## Bmal1 Overexpression Reduces M1 Macrophage Markers and Inflammatory Cytokine Secretion in RAW264.7 Cells

To further investigate the role of Bmal1 in macrophage polarization, RAW264.7 cells were stimulated with LPS (100 ng/mL for 24 h) to induce the M1 phenotype or IL-4 (10 ng/mL) to induce M2 macrophages. Bmal1 mRNA expression was measured by qRT-PCR. IL-4 significantly increased Bmal1 mRNA expression in RAW264.7 cells, while LPS treatment reduced Bmal1 expression. After transfection with Bmal1 siRNA, Bmal1 mRNA expression was significantly reduced under IL-4 stimulation in RAW264.7 cells, with increased levels of NOS2 mRNA expression, pro-inflammatory cytokines TNF- $\alpha$  and IL-1 $\beta$  and decreased level of anti-inflammatory cytokine IL-10. In contrast, overexpression of Bmal1 (Bmal1-OE) significantly increased Bmal1 expression under LPS stimulation, with reduced NOS2 mRNA expression, TNF- $\alpha$  and IL-1 $\beta$  and increased IL-10 (Figure 2A and B). Flow cytometry analysis confirmed that Bmal1 overexpression significantly decreased CD86 expression under LPS stimulation, while Bmal1 knockdown decreased CD206 expression under IL-4 stimulation (Figure 2C). Immunofluorescence staining revealed that Bmal1 overexpression significantly reduced NOS2 fluorescence in LPS-treated cells, while Bmal1 interference reduced CD206 fluorescence under IL-4 treatment (Figure 2D). These findings suggested that Bmal1 modulates macrophage phenotypic alterations.

## Bmal1 Interference Alters Sirt1 Expression and NF- $\kappa$ B Signaling Pathway in RAW264.7 Cells

RAW264.7 cells were stimulated with IL-4 (10 ng/mL for 24 h) to induce M2 macrophages. To assess the impact of Bmal1 knockdown on gene expression, Bmal1 siRNA treatment was performed, and gene expression profiles were analyzed by high-throughput transcriptome sequencing (Figure 3A and B). KEGG analysis revealed significantly altered pathways including Herpes simplex virus 1 infection, cell cycle, cytokine-cytokine receptor interaction, TNF signaling pathway, hematopoietic cell lineage, p53 signaling pathway, NF- $\kappa$ B signaling pathway, genes related to rheumatoid arthritis and other signaling pathways (Figure 3C). Heatmap analysis showed a significant up-regulation of NOS2 and down-regulation of Sirt1 (Figure 3D and E).

## Bmal1 Positively Regulates Sirt1 Expression

The intersection of genes transcriptionally regulated by Bmal1 from a transcription factor database and down-regulated genes identified in transcriptome sequencing was obtained to identify genes which are direct targets of Bmal1. A total of 76 overlapping genes were identified, including Sirt1 (Figure 4A). The specific binding site of Bmal1 on the Sirt1 promoter was predicted using the JASPAR database. A Bmal1 binding site (ACTCTCGTGC) was identified within the Sirt1 promoter at -943 to -934 bp relative to the transcription start site (Figure 4B). ChIP assay confirmed Bmal1 directly binding to the Sirt1 promoter (Figure 4C). The effect of Bmal1 on Sirt1 promoter activity was validated through a dual-luciferase reporter assay. Bmal1 overexpression increased the luciferase activity of the plasmid containing the complete sequence of the Sirt1 promoter. In contrast, Bmal1 overexpression could not increase the luciferase activity of plasmids containing promoter fragments of Sirt1 (Figure 4D). PCR analysis confirmed that Bmal1 overexpression significantly increased Sirt1 expression, while Bmal1 interference reduced Sirt1 expression (Figure 4E). Notably, the post-transcriptional modifications of RelA/p65 are critical for NF- $\kappa$ B transcriptional activity.<sup>33</sup> Specifically, RelA/p65 Ser536 is a key phosphorylation site that can be phosphorylated by various kinases in response to stimuli,<sup>34</sup> and its phosphorylation is critical for NF- $\kappa$ B activation and downstream inflammatory responses. Therefore, Ser536 phosphorylation of p65 was examined in this study. Western blot analysis further confirmed that Bmal1 overexpression increased Sirt1 expression and reduced NOS2 expression and the p-p65/p65 ratio, indicating inhibition of NF- $\kappa$ B signaling. In contrast, Bmal1 interference led to the opposite effects (Figure 4F).

## Sirt1 Knockdown Partially Reverses the Inhibitory Effect of Bmal1 on M1 Macrophage Polarization

Three siRNAs targeting Sirt1 (siSirt1-1, siSirt1-2, and siSirt1-3) were designed and evaluated for knockdown efficiency. Among them, siSirt1-2 exhibited the highest silencing efficiency at both the mRNA and protein levels, with reductions of

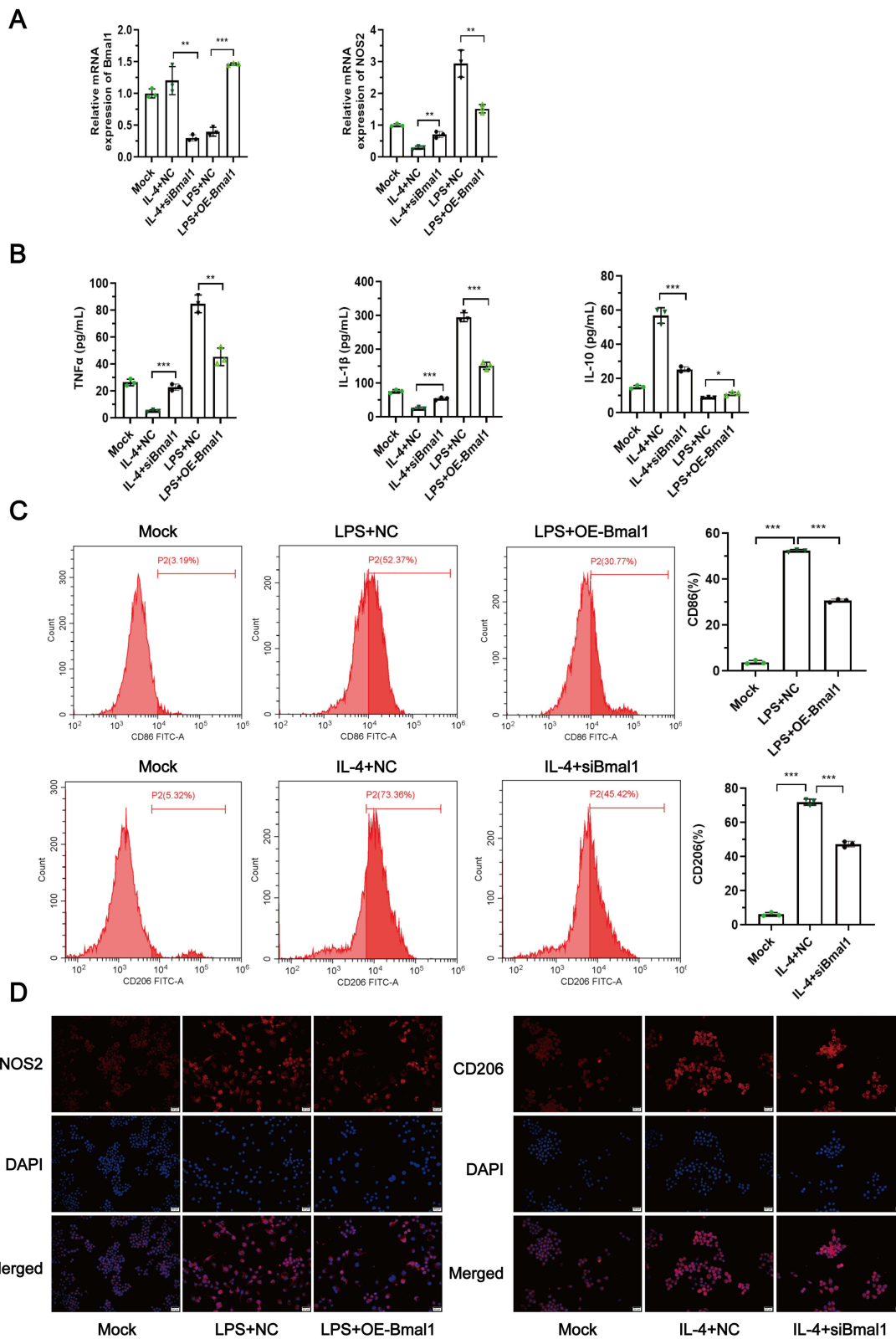


**Figure 2** Bmal1 overexpression reduces M1 macrophage markers and inflammatory factors secretion in RAW264.7 cells. **(A)** Bmal1 and NOS2 mRNA expression were analyzed by qRT-PCR. **(B)** Levels of TNF- $\alpha$ , IL-1 $\beta$  and IL-10 were determined by ELISA. **(C)** CD86 and CD206 levels were detected by flow cytometry. **(D)** Immunofluorescence labeling analysis was applied to manifest the presence of NOS2 and CD206. Experiments in **A** and **B** were performed with 3 technical replicates. Experiment in **D** was performed using 3 randomly selected fields per sample. Sample size: n = 3 independent biological replicates per group (**A–D**). Data are presented as mean  $\pm$  SEM. Scale bar: 20  $\mu$ m. \*P < 0.05, \*\*P < 0.01, \*\*\*P < 0.001. P values < 0.05 were considered significant.

**Abbreviations:** Bmal1, brain and muscle Arnt-like protein-1; IL-1 $\beta$ , interleukin-1 $\beta$ ; IL-4, interleukin-4; IL-10, interleukin-10; LPS, lipopolysaccharide; NOS2, nitric oxide synthase2; TNF- $\alpha$ , tumor necrosis factor-alpha.



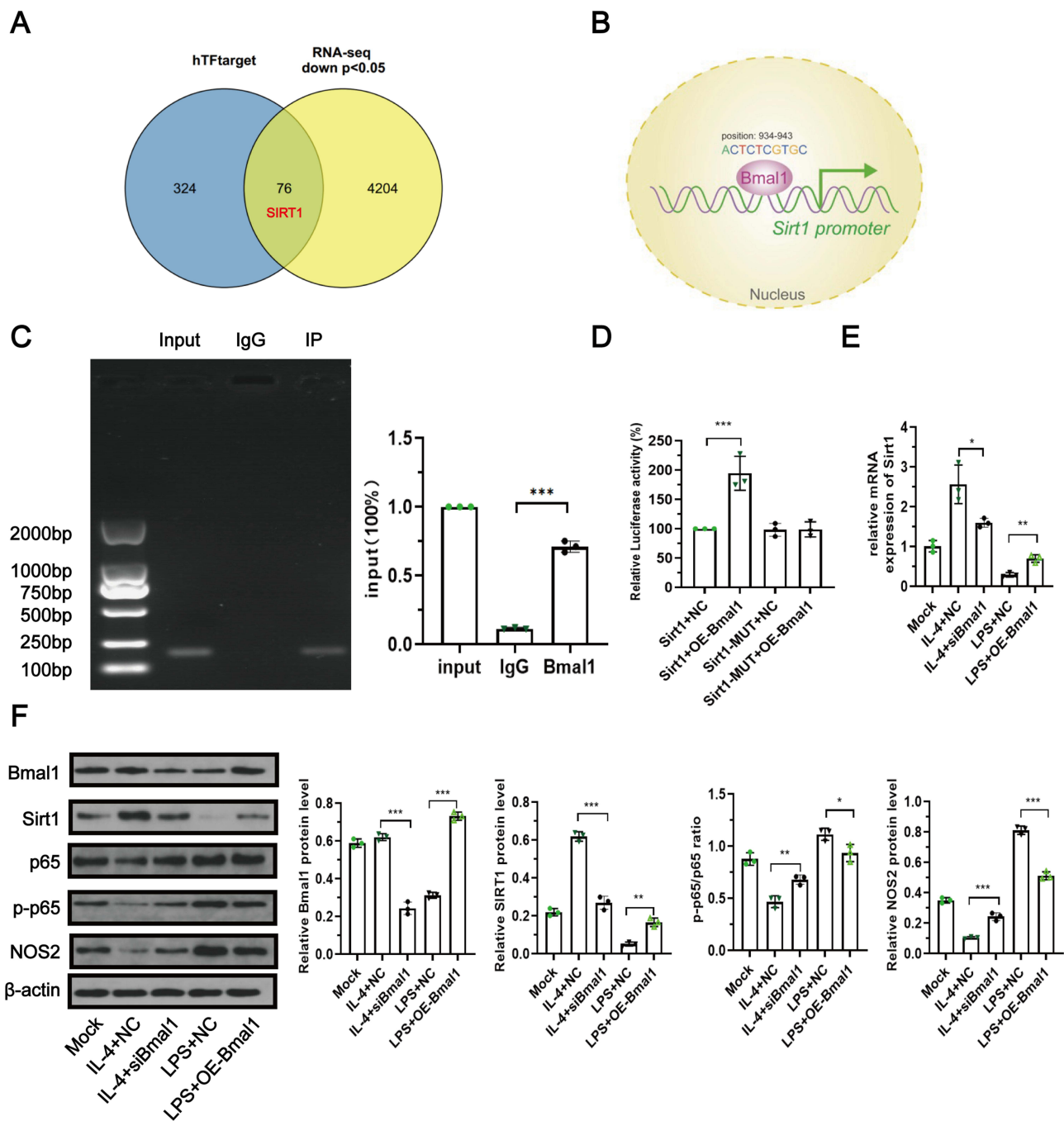


**Figure 4** Bmal1 positively regulates Sirt1 expression. **(A)** The intersection of genes transcriptionally regulated by Bmal1 from a transcription factor database and downregulated genes identified in transcriptome sequencing were analyzed. **(B)** The specific binding site of Bmal1 on the Sirt1 promoter was predicted using the JASPAR database. **(C)** Chromatin immunoprecipitation (ChIP) was used to confirm the direct binding of Bmal1 to the Sirt1 promoter. **(D)** The effect of Bmal1 on Sirt1 promoter activity was validated through a dual-luciferase reporter assay. **(E)** Sirt1 mRNA expression were analyzed by qRT-PCR. **(F)** Bmal1, Sirt1, p65, p-p65 and NOS2 protein expression were analyzed by Western blot. Experiments in **C** and **E** were performed with 3 technical replicates. Sample size:  $n = 3$  independent biological replicates per group (**C-F**). Data are presented as mean  $\pm$  SEM. \* $P < 0.05$ , \*\* $P < 0.01$ , \*\*\* $P < 0.001$ . P values  $< 0.05$  were considered significant.

**Abbreviations:** Bmal1, brain and muscle Arnt-like protein-1; NOS2, nitric oxide synthase2; p65, RelA; p-p65, phosphorylated p65; Sirt1, Sirtuin-1.

## Bmal1 Overexpression Attenuates Arthritis Severity and Inhibits the Inflammatory Responses in CIA Mice

Two lentiviral vectors carrying Bmal1 were designed and evaluated for their overexpression efficiency. OE-Bmal1-2 exhibited higher overexpression efficiency at both the mRNA and protein levels, showing a 3.58-fold increase in Bmal1

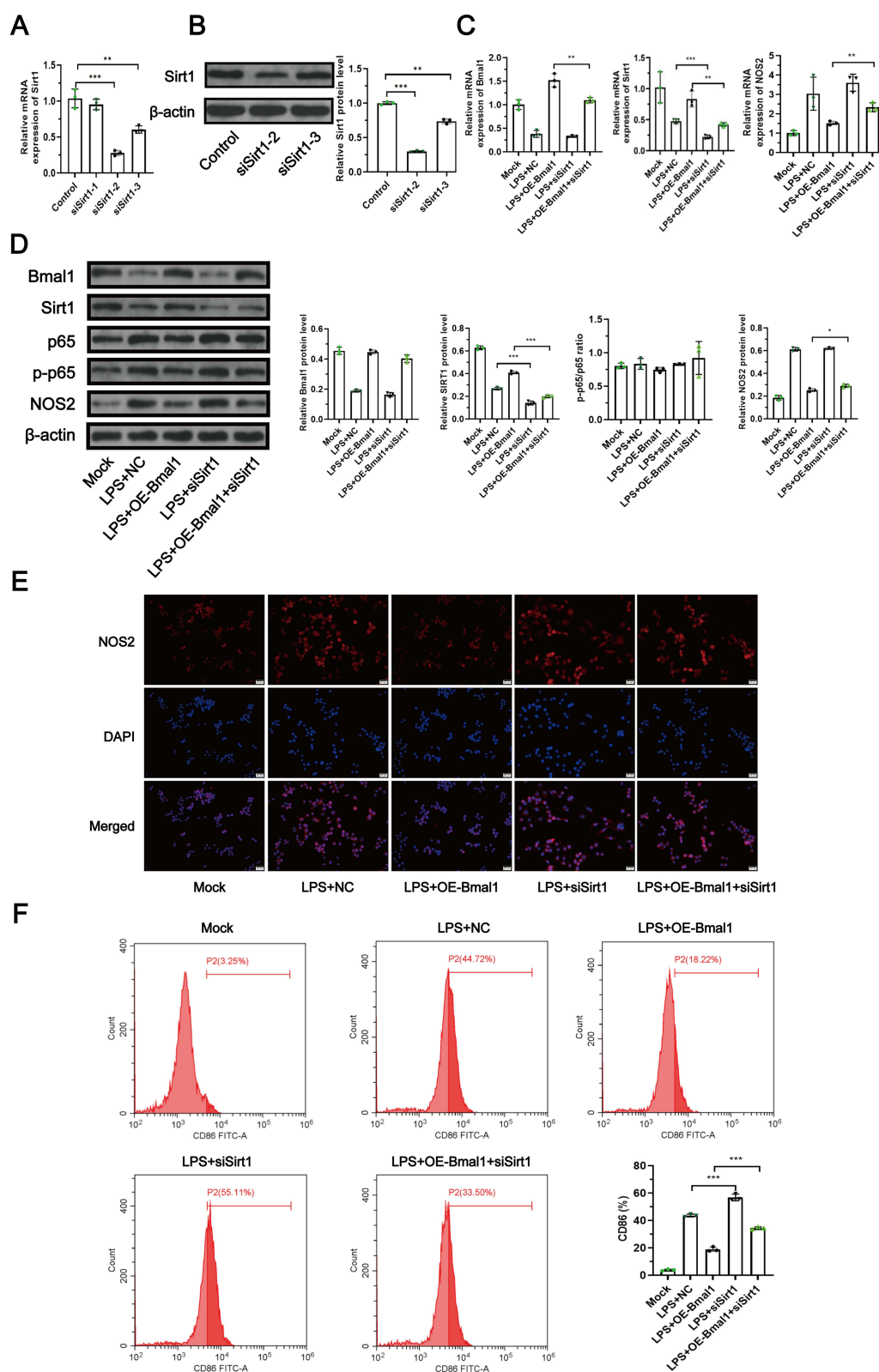


**Figure 5** Sirt1 is involved in the process of Bmal1-mediated regulation of macrophage phenotypic alteration. **(A)** Knockdown efficiency of Sirt1 was evaluated at the mRNA levels by qRT-PCR. **(B)** Knockdown efficiency of Sirt1 was evaluated at protein levels by Western blot. **(C)** Bmal1, Sirt1 and NOS2 mRNA expression were analyzed by qRT-PCR. **(D)** Bmal1, Sirt1, p65, p-p65 and NOS2 protein expression were analyzed by Western blot. **(E)** Immunofluorescence labeling analysis was applied to manifest the presence of NOS2. **(F)** The level of CD86 was detected by flow cytometry. Experiments in **A** and **C** were performed with 3 technical replicates. Experiment in **E** was performed using 3 randomly selected fields per sample. Sample size:  $n = 3$  independent biological replicates per group (**A–F**). Data are presented as mean  $\pm$  SEM. Scale bar: 20  $\mu$ m. \* $P < 0.05$ , \*\* $P < 0.01$ , \*\*\* $P < 0.001$ . P values  $< 0.05$  were considered significant.

**Abbreviations:** Bmal1, brain and muscle Arnt-like protein-1; NOS2, nitric oxide synthase2; p65, RelA; p-p65, phosphorylated p65; Sirt1, Sirtuin-1.

mRNA (qPCR) and a 3.30-fold increase in Bmal1 protein (immunofluorescence analysis) (Figure 6A and B), and was therefore selected for subsequent experiments. To further investigate the role of Bmal1 in RA, a CIA mouse model was established. As expected, the CIA mice developed red, swollen paws accompanied by higher arthritis scores, which are characteristic features of RA (Figure 6C). HE staining was performed to assess the histopathological changes in the knee joints. As anticipated, inflammatory cell infiltration, synovial hyperplasia, joint space narrowing and bone erosion were observed in the joint tissues of CIA mice (Figure 6D). CIA mice overexpressing Bmal1 exhibited markedly reduced clinical symptoms and arthritis scores (Figure 6C). In addition, Bmal1 overexpression attenuated inflammatory cell infiltration, synovial hyperplasia and bone erosion (Figure 6D). Moreover, compared with CIA mice, those overexpressing Bmal1 showed lower levels of TNF- $\alpha$  and IL-1 $\beta$  and a higher level of IL-10 (Figure 6E).

## Bmal1 Overexpression Increases Sirt1 Expression and Inhibits M1 Macrophage Polarization in CIA Mice

In line with the clinical and in vitro data, Bmal1 protein expression was significantly reduced in the synovial tissues of CIA mice compared with controls, accompanied by down-regulation of Sirt1 expression, an increased p-p65/p65 ratio and elevated NOS2 expression. Moreover, Bmal1 overexpression in CIA mice partially reversed these changes (Figure 7A). Immunofluorescence double-labeling analysis was performed to examine the co-expression of Bmal1 with the macrophage marker F4/80 and NOS2, as well as the co-expression of CD206 with NOS2 in synovial tissues. Reduced Bmal1 fluorescence was observed in CIA mice, whereas it was increased in CIA mice overexpressing Bmal1 (Figure 7B). CIA mice also exhibited increased NOS2, which was partially reversed by Bmal1 overexpression (Figure 7C). Further quantitative analysis of immunofluorescence staining demonstrated a significant decrease in NOS2-positive macrophages and a concomitant increase in CD206-positive macrophages following Bmal1 overexpression, suggesting a shift toward an M2-like macrophage phenotype in vivo (Figure 7D).

## Discussion

RA is a chronic autoimmune disease that primarily affects the joints, leading to persistent inflammation and joint damage.<sup>1</sup> Loss of Bmal1 leads to joint and synovial lesion. Col6a1-Bmal1<sup>-/-</sup> mice exhibit abnormalities in ankle joint architecture, such as synovial thickening and osteophyte formation.<sup>35</sup> Moreover, Bmal1 deficiency in fibroblast-like synoviocytes (FLS) enhances the secretion of pro-inflammatory cytokines while reducing anti-inflammatory cytokine levels.<sup>35</sup> However, the functional role of Bmal1 in RA remains largely unexplored. In our study, we observed that Bmal1 expression was significantly reduced in the synovial tissues of RA patients, which was confirmed by the GEO dataset GSE55235. Furthermore, Bmal1 mRNA levels were increased in PBMCs of RA patients after MTX treatment. In parallel, Bmal1 expression was down-regulated in CIA mice (an animal model of RA), and Bmal1 overexpression in these mice significantly alleviated clinical manifestations and reduced arthritis scores, suggesting a potential regulatory role of Bmal1 in RA. This finding aligns with previous observations in malignancies, where Bmal1 acts as a tumor suppressor gene,<sup>36</sup> and its overexpression inhibits melanoma cell proliferation.<sup>37</sup> Interestingly, some studies have reported increased Bmal1 expression in RA synovial tissues,<sup>26,27</sup> which appears inconsistent with our findings. Several factors may contribute to this discrepancy. One possible explanation is that the cellular heterogeneity of synovial tissues plays an important role. Prior studies have largely focused on FLS,<sup>35</sup> whereas the present study primarily investigated macrophage polarization and inflammatory responses. As Bmal1 may exert cell-type-specific regulatory effects, its expression pattern and functional consequences could differ between synovial fibroblasts and immune cells. Another contributing factor is that disease stage and medication exposure may influence circadian gene expression. Patients with RA often receive disease-modifying antirheumatic drugs (DMARDs), glucocorticoids, or other immunomodulatory therapies, which may alter inflammatory signaling and potentially affect circadian regulators such as Bmal1. In addition, the circadian nature of clock genes should also be considered. The expression of Bmal1 oscillates over the circadian cycle, and variations in sampling time across studies may lead to differences in the measured expression levels. Taken together, these factors may partially explain the divergent observations across studies and highlight the complexity of circadian regulation in RA pathogenesis.

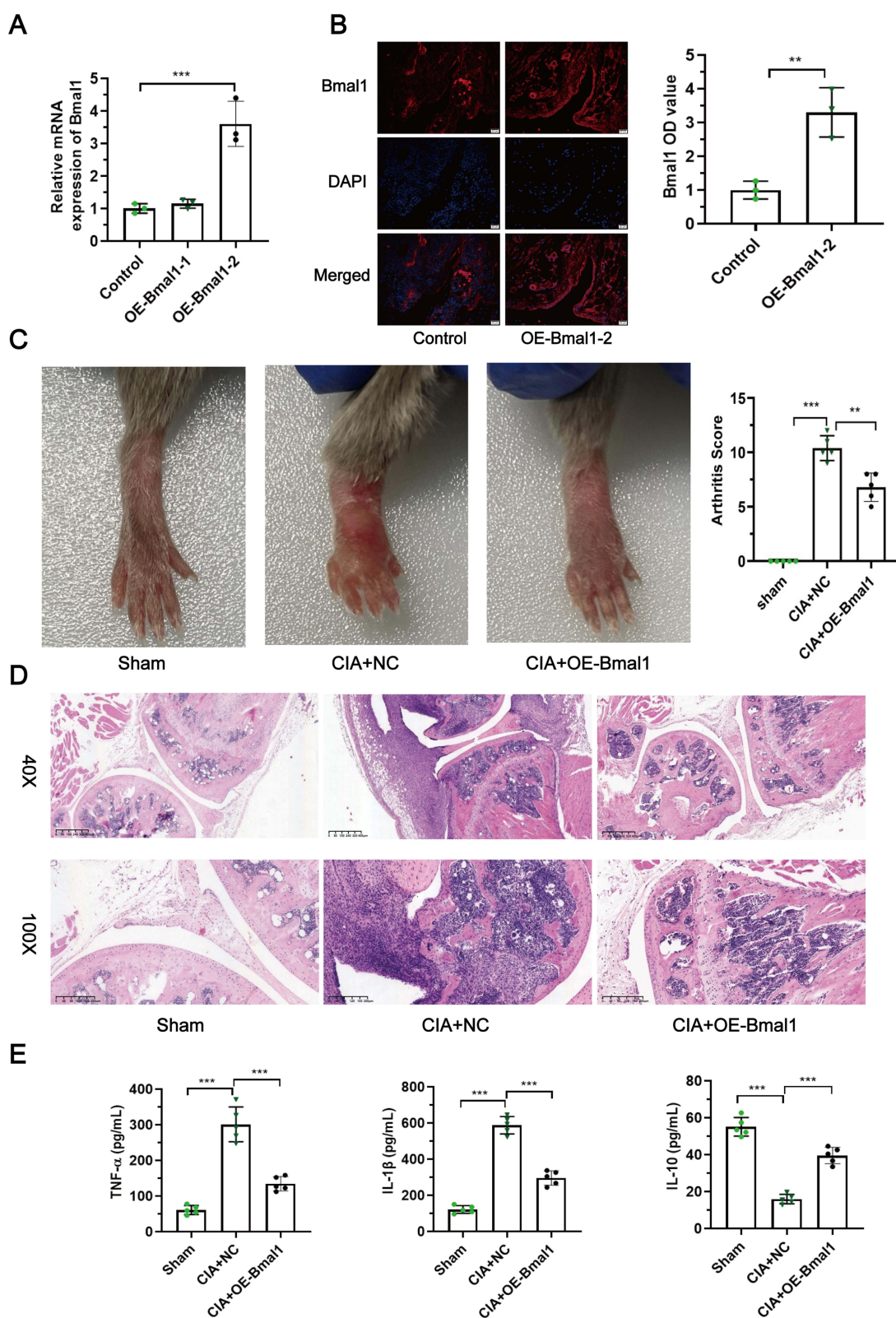


**Figure 6** Bmal1 overexpression attenuates arthritis severity in CIA mice. **(A)** Overexpression efficiency of Bmal1 was evaluated at the mRNA levels by qRT-PCR. **(B)** Overexpression efficiency of Bmal1 was evaluated at protein levels by immunofluorescence analysis. Quantification of Bmal1 protein expression was presented as optical density (OD) values. **(C)** Clinical arthritis was evaluated by examination of swelling and redness of the paws. Arthritis scores were analyzed in mice. **(D)** HE staining of the knee joints in mice. **(E)** Levels of TNF- $\alpha$ , IL-1 $\beta$  and IL-10 in serum of mice were determined by ELISA. In **(B)**, 3 randomly selected fields per sample were analyzed. Experiments in **(A)** and **(E)** were performed with 3 technical replicates. Sample size:  $n = 3$  independent biological replicates per group **(A)** and **(B)** and  $n = 5$  independent biological replicates per group **(C–E)**. Data are presented as mean  $\pm$  SEM. Scale bars: 20  $\mu$ m **(B)**; 400  $\mu$ m ( $\times 40$ ) and 200  $\mu$ m ( $\times 100$ ) **(D)**. \*\* $P < 0.01$ , \*\*\* $P < 0.001$ .  $P$  values  $< 0.05$  were considered significant.

**Abbreviations:** Bmal1, brain and muscle Arnt-like protein-1; CIA mice, collagen-induced arthritis mice; IL-1 $\beta$ , interleukin-1 $\beta$ ; IL-10, interleukin-10; TNF- $\alpha$ , tumor necrosis factor-alpha.

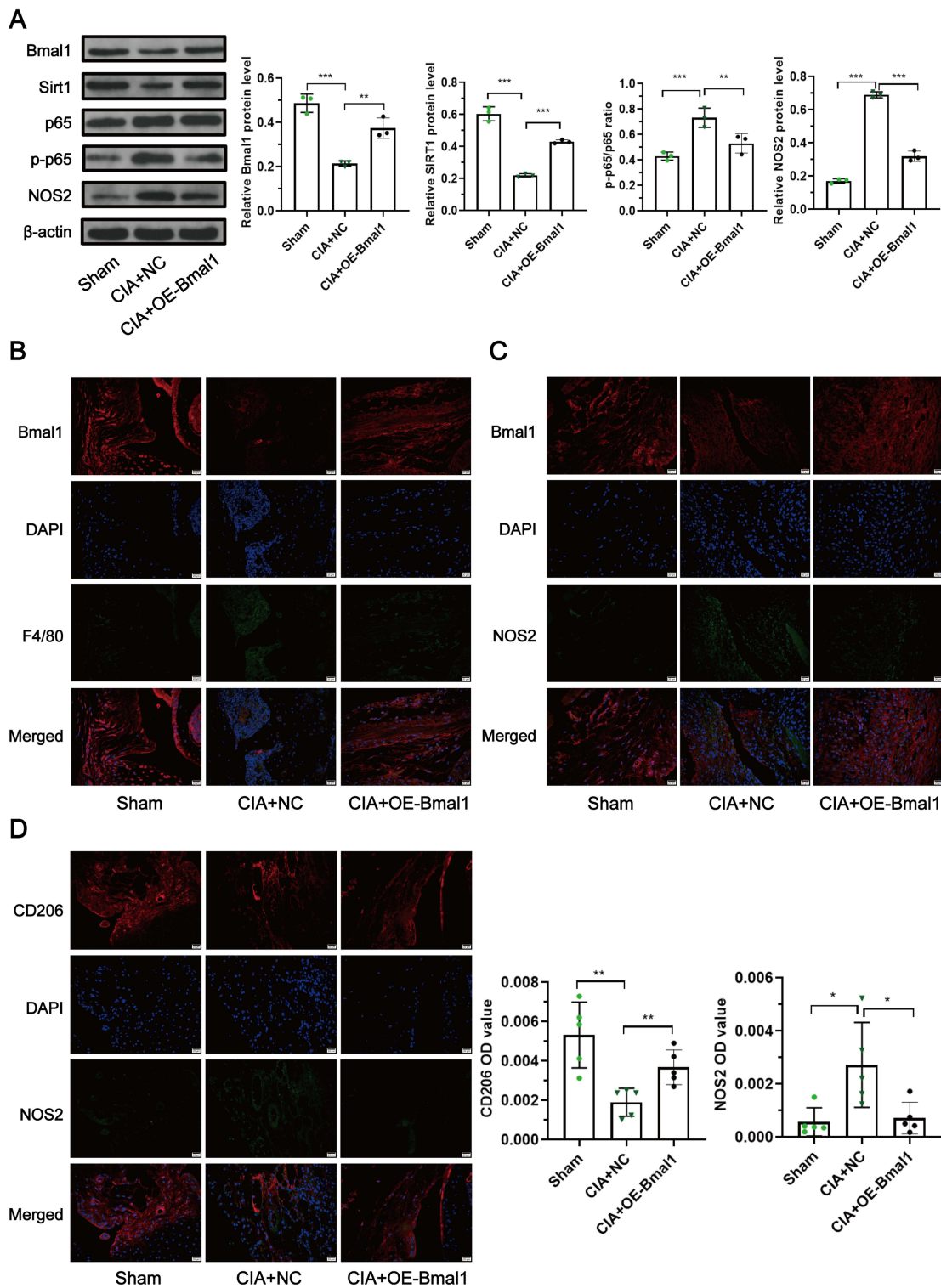


**Figure 7** Bmal1 overexpression reduces M1 macrophage markers in the knee joints in CIA mice. **(A)** Bmal1, Sirt1, p65, p-p65 and NOS2 protein expression were analyzed in synovial tissues by Western blot. **(B)** Immunofluorescence double labeling analysis was applied to manifest the presence of Bmal1 (red) co-expression with F4/80 (green) in synovial tissues. **(C)** Immunofluorescence double labeling analysis was applied to manifest the presence of Bmal1 (red) co-expression with NOS2 (green) in synovial tissues. **(D)** Immunofluorescence double labeling analysis was applied to manifest the presence of CD206 (red) co-expression with NOS2 (green) in synovial tissues. CD206 and NOS2 protein expression was quantified as optical density (OD) values. In **B–D**, 3 randomly selected fields per sample were analyzed. Sample size:  $n = 3$  (**A**) and  $n = 5$  independent biological replicates per group (**B–D**). Data are presented as mean  $\pm$  SEM. Scale bar: 20  $\mu$ m (**B–D**). \*P < 0.05, \*\*P < 0.01, \*\*\*P < 0.001. P values < 0.05 were considered significant. **Abbreviations:** Bmal1, brain and muscle Arnt-like protein-1; F4/80, epidermal growth factor (EGF)-like module-containing mucin-like hormone receptor-like 1; NOS2, nitric oxide synthase2; p65, RelA; p-p65, phosphorylated p65; Sirt1, Sirtuin-1.

Macrophages are key immune cells involved in maintaining tissue homeostasis and orchestrating immune responses.<sup>5</sup> Dysregulation of macrophage polarization, particularly an imbalance between pro-inflammatory M1 and anti-inflammatory M2 macrophages, has been implicated in RA pathogenesis.<sup>38</sup> Analysis of the GSE55235 dataset indicated a potential shift in the correlation between Bmal1 expression and M2 marker scores in RA compared with controls, providing exploratory evidence for a possible association between Bmal1 and macrophage polarization. In the present study, Bmal1 overexpression in CIA mice and LPS-treated RAW264.7 cells attenuated M1 macrophage markers while promoting M2 markers, suggesting a role for Bmal1 in regulating macrophage polarization and mitigating inflammation in RA.

Consistent with these findings, previous studies have shown that Bmal1 knockdown induces M1 polarization and inhibits M2 polarization in glioblastoma cells,<sup>39</sup> while its down-regulation promotes pro-inflammatory factors in HK-2 cells and mouse kidney tissues.<sup>40</sup> NF- $\kappa$ B signaling plays a central role in macrophage polarization and inflammation in RA, and its inhibition reduces inflammatory cytokine production and joint damage.<sup>41,42</sup> Accordingly, our results demonstrated that Bmal1 overexpression suppressed NF- $\kappa$ B activation in both CIA mice and LPS-stimulated RAW264.7 cells, further supporting its role in regulating macrophage polarization and inflammatory responses.

Sirt1 regulates the activity of various transcription factors including NF- $\kappa$ B.<sup>43</sup> Our findings suggested that Sirt1 was a key mediator of Bmal1-driven regulation of macrophage polarization and inflammatory responses. Moreover, Bmal1 appears to positively regulate Sirt1 expression both in vivo and in vitro, supporting a functional link between these two molecules. Additionally, Bmal1 have been shown to shape immune cell metabolism and thereby influence inflammatory responses.<sup>17,20</sup> Given the central role of Sirt1 in metabolic regulation,<sup>24</sup> these findings suggest that Bmal1 may influence macrophage polarization partly through immunometabolic pathways. Bioinformatic prediction and experimental validation further indicate that Sirt1 may be a direct transcriptional target of Bmal1, highlighting a potential mechanism by which Bmal1 modulates downstream signaling pathways. Functionally, the Sirt1/NF- $\kappa$ B axis likely represents an important pathway through which Bmal1 suppresses M1 macrophage polarization and inflammation. However, given that Sirt1 inhibition only partially attenuated the effects of Bmal1, it is plausible that additional signaling pathways are also involved. In line with this, transcriptomic analysis indicates broader regulatory changes, suggesting that Bmal1 may exert its effects through a complex network of downstream targets rather than a single pathway.

To our knowledge, this is the first study to demonstrate a protective role of Bmal1 overexpression in RA. Given the lack of macrophage-targeted therapies for RA, Bmal1 may represent a promising therapeutic target, potentially modulated through circadian regulatory pathways. Notably, REV-ERB $\alpha$ , a nuclear receptor within the Bmal1 network, can be targeted by agonists such as SR9009 to suppress macrophage inflammation in a Bmal1-dependent manner.<sup>44</sup> However, several challenges remain. As the circadian clock is a systemic network, global modulation of Bmal1 may lead to unintended effects on metabolism and sleep–wake cycles.<sup>45</sup> Meanwhile, currently available circadian-targeting compounds remain largely at the preclinical stage, with their long-term safety yet to be established. Therefore, further studies are required to optimize specificity and safety for clinical application.

Despite the strengths of this study, several limitations should be acknowledged. First, the relatively small sample size of RA patients may limit statistical power. In addition, patients were receiving glucocorticoids and DMARDs, which may influence inflammatory status and gene expression profiles. Moreover, analyses based on PBMCs are subject to cellular heterogeneity, and treatment-induced changes in cell composition may confound the interpretation of Bmal1 expression, highlighting the need for studies using purified immune cell subsets or single-cell approaches. Second, our experimental findings rely on the RAW264.7 macrophage cell line and CIA model, which may not fully recapitulate the complexity of human RA. Validation in primary human cells and humanized models would strengthen translational relevance. Third, while this study focused on macrophage polarization, RA pathogenesis involves multiple immune cell types, and the role of circadian regulation in other immune populations remains to be elucidated. In addition, although NF- $\kappa$ B signaling was implicated, its activation was primarily assessed by p65 phosphorylation and downstream cytokines, and more comprehensive analyses (eg, I $\kappa$ B $\alpha$  degradation or nuclear translocation assays) are warranted. Finally, circadian time-of-day effects were not controlled during sample collection. Therefore, further studies incorporating circadian-controlled designs and clinical validation in larger patient cohorts are required to substantiate the therapeutic potential of Bmal1 modulation in RA.

## Conclusion

In conclusion, our study provides strong evidence that Bmal1 is a critical regulator of macrophage polarization in RA. Local overexpression of Bmal1 is associated with enhanced M2 polarization through modulation of the Sirt1/NF- $\kappa$ B axis, thereby suppressing pro-inflammatory responses and alleviating synovitis. These findings deepen our understanding of RA pathogenesis and suggest that Bmal1 may represent a clinically actionable target for macrophage-focused therapies. However, as these findings are primarily based on preclinical models, further validation in larger patient cohorts is required. Future studies should place particular emphasis on stratification by cell type, given the cell-type-specific functions of Bmal1 across synovial cell populations including macrophages and other immune cells. In addition, considering the circadian nature of clock genes, stratification by sampling time and the incorporation of time-course analyses will be essential to accurately define the temporal dynamics of Bmal1 in RA.

## Data Sharing Statement

The data used during the current study are available from the corresponding author on reasonable request.

## Ethics Approval

Ethical approval was obtained from the Ethics Committee of the Second Affiliated Hospital of Zhejiang University School of Medicine (approval numbers: 2024-184 and 2025-0681). The authors confirm that the animal study have adhered to the ARRIVE guidelines.

## Acknowledgments

The authors thank the patients who donated samples. The authors thank Lingjiang Zhu and the doctors (Second Affiliated Hospital of Zhejiang University School of Medicine) for their assistance in acquiring the synovial tissue samples.

## Author Contributions

Huaxiang Wu contributed to conceptualization, project administration, writing–review and editing. Weihong Xu contributed to conceptualization, resources, supervision, writing–review and editing. Lu Ye contributed to conceptualization, funding acquisition, supervision and writing–original draft. Xiaomei Wang contributed to formal analysis, investigation, methodology and validation, writing–review and editing. All authors have agreed on the journal to which the article will be submitted, gave final approval of the version to be published, and agree to be accountable for all aspects of the work.

## Funding

This work was supported by the National Natural Science Foundation of China (NO. 82302021).

## Disclosure

The authors report no conflicts of interest in this work.

## References

1. Sparks JA. Rheumatoid Arthritis. *Ann Intern Med.* 2019;170(1):Itc1–itc16. doi:10.7326/AITC201901010
2. Brown P, Pratt AG, Hyrich KL. Therapeutic advances in rheumatoid arthritis. *BMJ.* 2024;384:e070856. doi:10.1136/bmj-2022-070856
3. Cutolo M, Campitiello R, Gotelli E, Soldano S. The role of M1/M2 macrophage polarization in rheumatoid arthritis synovitis. *Front Immunol.* 2022;13:867260. doi:10.3389/fimmu.2022.867260
4. Chen S, Saeed AFUH, Liu Q, et al. Macrophages in immunoregulation and therapeutics. *Signal Transduct Target Ther.* 2023;8(1):207. doi:10.1038/s41392-023-01452-1
5. Rodríguez-Morales P, Franklin RA. Macrophage phenotypes and functions: resolving inflammation and restoring homeostasis. *Trends Immunol.* 2023;44(12):986–998. doi:10.1016/j.it.2023.10.004
6. Yunna C, Mengru H, Lei W, Weidong C. Macrophage M1/M2 polarization. *Eur J Pharmacol.* 2020;877:173090. doi:10.1016/j.ejphar.2020.173090
7. Raveenthiraraj S, Awanis G, Chieppa M, O'Connell AE, Sobolewski A. M1 and M2 macrophages differentially regulate colonic crypt renewal. *Inflamm Bowel Dis.* 2024;30(7):1138–1150. doi:10.1093/ibd/izad270
8. Zhang Z, Zhang R, Li L, et al. Macrophage migration inhibitory factor (MIF) inhibitor, Z-590 suppresses cartilage destruction in adjuvant-induced arthritis via inhibition of macrophage inflammatory activation. *Immunopharmacol Immunotoxicol.* 2018;40(2):149–157. doi:10.1080/08923973.2018.1424896

9. Wilantri S, Grasshoff H, Lange T, Gaber T, Besedovsky L, Buttgerit F. Detecting and exploiting the circadian clock in rheumatoid arthritis. *Acta Physiol.* 2023;239(2):e14028. doi:10.1111/apha.14028
10. Xiang K, Xu Z, Hu YQ, et al. Circadian clock genes as promising therapeutic targets for autoimmune diseases. *Autoimmun Rev.* 2021;20(8):102866. doi:10.1016/j.autrev.2021.102866
11. Xu H, Huang L, Zhao J, Chen S, Liu J, Li G. The circadian clock and inflammation: a new insight. *Clin Chim Acta.* 2021;512:12–17. doi:10.1016/j.cca.2020.11.011
12. Lee H, Nah SS, Chang SH, et al. PER2 is downregulated by the LPS-induced inflammatory response in synoviocytes in rheumatoid arthritis and is implicated in disease susceptibility. *Mol Med Rep.* 2017;16(1):422–428. doi:10.3892/mmr.2017.6578
13. Butler T, Maidstone JR, Rutter KM, McLaughlin TJ, Ray WD, Gibbs EJ. The associations of chronotype and shift work with rheumatoid arthritis. *J Biol Rhythms.* 2023;38(5):510–518. doi:10.1177/07487304231179595
14. Haas S, Straub RH. Disruption of rhythms of molecular clocks in primary synovial fibroblasts of patients with osteoarthritis and rheumatoid arthritis, role of IL-1 $\beta$ /TNF. *Arthritis Res Ther.* 2012;14(3):R122. doi:10.1186/ar3852
15. Ferrell JM. Circadian rhythms and inflammatory diseases of the liver and gut. *Liver Res.* 2023;7(3):196–206. doi:10.1016/j.livres.2023.08.004
16. Xie M, Tang Q, Nie J, et al. BMAL1-downregulation aggravates porphyromonas gingivalis-induced atherosclerosis by encouraging oxidative stress. *Circ Res.* 2020;126(6):e15–e29. doi:10.1161/CIRCRESAHA.119.315502
17. Schrader LA, Ronnekleiv-Kelly SM, Hogenesch JB, Bradfield CA, Malecki KM. Circadian disruption, clock genes, and metabolic health. *J Clin Invest.* 2024;134(14):e170998. doi:10.1172/JCI170998
18. Kaneshiro K, Nakagawa K, Tsukamoto H, et al. The clock gene Bmal1 controls inflammatory mediators in rheumatoid arthritis fibroblast-like synoviocytes. *Biochem Biophys Res Commun.* 2024;691:149315. doi:10.1016/j.bbrc.2023
19. Alexander RK, Liou YH, Knudsen NH, et al. Bmal1 integrates mitochondrial metabolism and macrophage activation. *eLife.* 2020;9:e54090. doi:10.7554/eLife.54090
20. Zhou Y, Wu M, Xu L, et al. Bmal1 regulates macrophage polarize through glycolytic pathway in alcoholic liver disease. *Front Pharmacol.* 2021;12:640521. doi:10.3389/fphar.2021.640521
21. He S, Wang Y, Liu J, Li P, Luo X, Zhang B. Activating SIRT1 deacetylates NF- $\kappa$ B p65 to alleviate liver inflammation and fibrosis via inhibiting NLRP3 pathway in macrophages. *Int J Med Sci.* 2023;20(4):505–519. doi:10.7150/ijms.77955
22. Yang F, Yan J, Lu Y, Wang D, Liu L, Wang Z. MicroRNA-499-5p targets SIRT1 to aggravate lipopolysaccharide-induced acute lung injury. *Free Radic Res.* 2021;55(1):71–82. doi:10.1080/10715762.2020
23. Liu X, Chen A, Liang Q, et al. Spermidine inhibits vascular calcification in chronic kidney disease through modulation of SIRT1 signaling pathway. *Aging Cell.* 2021;20(6):e13377. doi:10.1111/ace1.13377
24. Aggarwal S, Trehanpati N, Nagarajan P, Ramakrishna G. The Clock-NAD<sup>+</sup> -Sirtuin connection in nonalcoholic fatty liver disease. *J Cell Physiol.* 2022;237(8):3164–3180. doi:10.1002/jcp.30772
25. He X, Yu M, Zhao J, et al. Chrono-moxibustion adjusts circadian rhythm of CLOCK and BMAL1 in adjuvant-induced arthritic rats. *Am J Transl Res.* 2022;14(7):4880–4897.
26. Kouri VP, Olkkonen J, Kaivosoja E, et al. Circadian timekeeping is disturbed in rheumatoid arthritis at molecular level. *PLoS One.* 2013;8(1):e54049. doi:10.1371/journal.pone.0054049
27. Yoshida K, Nakai A, Kaneshiro K, et al. TNF- $\alpha$  induces expression of the circadian clock gene Bmal1 via dual calcium-dependent pathways in rheumatoid synovial cells. *Biochem Biophys Res Commun.* 2018;495:1675–1680. doi:10.1016/j.bbrc.2017.12.015
28. Arnett FC, Edworthy SM, Bloch DA, et al. The American rheumatism association 1987 revised criteria for the classification of rheumatoid arthritis. *Arthritis Rheum.* 1988;31(3):315–324. doi:10.1002/art.1780310302
29. Aletaha D, Neogi T, Silman AJ, et al. 2010 rheumatoid arthritis classification criteria: an American College of Rheumatology/European league against rheumatism collaborative initiative. *Arthritis Rheum.* 2010;62(9):2569–2581. doi:10.1002/art.27584
30. Altman R, Asch E, Bloch D, et al; Diagnostic and Therapeutic Criteria Committee of the American Rheumatism Association. Development of criteria for the classification and reporting of osteoarthritis. Classification of osteoarthritis of the knee. *Arthritis Rheum.* 1986;29(8):1039–1049. doi:10.1002/art.1780290816
31. Liu X, Fang F, Duan H, Wu C, Liu H, Ding S. KLF11 alleviates rheumatoid arthritis by regulating M1 macrophage polarization via downregulation of YAP1 expression. *Arthritis Res Ther.* 2025;27(1):171. doi:10.1186/s13075-025-03634-4
32. Cheng Y, Zhu X, Wang X, et al. *Trichinella spiralis* infection mitigates collagen-induced arthritis via programmed death 1-mediated immunomodulation. *Front Immunol.* 2018;9:1566. doi:10.3389/fimmu.2018.01566
33. Wang C, Wang W, Hui X, et al. Case report and literature review: clinical manifestations and treatment of human RelA deficiency. *Front Immunol.* 2025;16:1529654. doi:10.3389/fimmu.2025.1529654
34. Zuo W, Ma H, Bi J, et al. Phosphorylation of RelA/p65 Ser536 inhibits the progression and metastasis of hepatocellular carcinoma by mediating cytoplasmic retention of NF- $\kappa$ B p65. *Gastroenterol Rep.* 2024;12:goae094. doi:10.1093/gastro/goae094
35. Hand LE, Dickson SH, Freemont AJ, Ray DW, Gibbs JE. The circadian regulator Bmal1 in joint mesenchymal cells regulates both joint development and inflammatory arthritis. *Arthritis Res Ther.* 2019;21(1):5. doi:10.1186/s13075-018-1770-1
36. Trebucq LL, Salvatore N, Wagner PM, Golombek DA, Chiesa JJ. Circadian clock gene bmal1 acts as a tumor suppressor gene in a mice model of human glioblastoma. *Mol Neurobiol.* 2024;61:5216–5229. doi:10.1007/s12035-023-03895-7
37. Lei T, Cai X, Zhang H, et al. Bmal1 upregulates ATG5 expression to promote autophagy in skin cutaneous melanoma. *Cell Signal.* 2024;124:111439. doi:10.1016/j.cellsig.2024.111439
38. Yang C, Ni B, Li C, et al. circRNA\_17725 promotes macrophage polarization towards M2 by targeting FAM46C to alleviate arthritis. *Mediators Inflamm.* 2023;6818524. doi:10.1155/2023/6818524
39. Wang F, Liao W, Li C, Zhu L. Silencing BMAL1 promotes M1/M2 polarization through the LDHA/lactate axis to promote GBM sensitivity to bevacizumab. *Int Immunopharmacol.* 2024;134:112187. doi:10.1016/j.intimp.2024.112187
40. Chen W, Zhao S, Xing J, et al. BMAL1 inhibits renal fibrosis and renal interstitial inflammation by targeting the ERK1/2/ELK-1/Egr-1 axis. *Int Immunopharmacol.* 2023;125(Pt B):111140. doi:10.1016/j.intimp.2023
41. Valeriano JDP, Andrade-Silva M, Pereira-Dutra F, et al. Cannabinoid receptor type 2 agonist GP1a attenuates macrophage activation induced by M. bovis -BCG by inhibiting NF- $\kappa$ B signaling. *J Leukoc Biol.* 2025;117(3):qiae246. doi:10.1093/jleuko/qiae246

42. Jimi E, Fei H, Nakatomi C. NF- $\kappa$ B signaling regulates physiological and pathological chondrogenesis. *Int J Mol Sci.* 2019;20(24):6275. doi:10.3390/ijms20246275
43. Zhao X, Li M, Lu Y, et al. and activating the Nrf2/HO-1 pathway. *Inflamm Res.* 2024;73(7):1173–1184. doi:10.1007/s00011-024-01890-9
44. Hong H, Cheung YM, Cao X, Wu Y, Li C, Tian XY. REV-ERB $\alpha$  agonist SR9009 suppresses IL-1 $\beta$  production in macrophages through BMAL1-dependent inhibition of inflammasome. *Biochem Pharmacol.* 2021;192:114701. doi:10.1016/j.bcp.2021.114701
45. Lee Y, Field JM, Sehgal A. Circadian rhythms, disease and chronotherapy. *J Biol Rhythms.* 2021;36(6):503–531. doi:10.1177/07487304211044301

Journal of Inflammation Research

Publish your work in this journal

The Journal of Inflammation Research is an international, peer-reviewed open-access journal that welcomes laboratory and clinical findings on the molecular basis, cell biology and pharmacology of inflammation including original research, reviews, symposium reports, hypothesis formation and commentaries on: acute/chronic inflammation; mediators of inflammation; cellular processes; molecular mechanisms; pharmacology and novel anti-inflammatory drugs; clinical conditions involving inflammation. The manuscript management system is completely online and includes a very quick and fair peer-review system. Visit <http://www.dovepress.com/testimonials.php> to read real quotes from published authors.

Submit your manuscript here: <https://www.dovepress.com/journal-of-inflammation-research-journal>

**Dovepress**  
Taylor & Francis Group